SILICON SOLAR CELL PARAMETERS CHANGE AFTER FOCUSED ION BEAM MILLING

Adam Gajdos

Doctoral Degree Programme (1), FEEC BUT

E-mail: xgajdo12@stud.feec.vutbr.cz

Supervised by: Pavel Skarvada

E-mail: skarvada@feec.vutbr.cz

Abstract: Silicon is still one of the most used materials for fabrication of solar cells. Some imperfections and defects may appear during production process. These local imperfections could be eliminated by focused ion beam (FIB). Nevertheless, FIB milling process modifies the crystal structure of the material by ions implantation. Samples under investigation are monocrystalline silicon solar cells. The impact of FIB milling is shown and discussed through current-voltage measurement before and after milling process.

Keywords: Silicon, solar cell, focused ion beam, I-V curve, SEM

1 INTRODUCTION

Silicon solar cell is essentially semiconductor device with large area *p-n* junction. Solar cell principle is based on the generation of electron-hole pairs and their separation by the junction built in potential [1]. Major interest of commercial production of solar cell still belongs to silicon photovoltaic technology [2]. Although they are reaching their theoretical limits, in commercial cells still exists some imperfections and defects that can lower the performance or shorten the life time. That is the motivation for investigation on silicon solar cells.

There are various natures of imperfections and defects such as inclusion, cracks, Schottky type shunts, structural defects [3]. Many techniques can be used for imperfections localization and detection [4], [5]. The presence of defect can be detected by electrical measurement, but this type of measurement does not give us information about defect location. Defect dimensions could range from atoms to orders of micrometers, consequently the localization of defects have to be provided by microscopic investigations as well as by defects light emission measurement under electrical bias conditions (applicable only for specific defects).

Investigated defect type can be localized accurately due to light emission in visible range under sample reversed bias condition. Different emission spectra of particular defects allow basic defect classification. For the purposes of this work it is more important that investigated defects start emit light at different reversed voltage value. For the purposes of light emission measurement optical far-field (high sensitive camera) or near-field (scanning near-field optical microscopy - SNOM) imaging can be used [6].

If defect is localized with methods mentioned earlier, it can be removed or isolated by focused ion beam (FIB) [7]. However, FIB modifies the surface by the ions of gallium or other liquid metal ion sources, as well as ion sources based on elemental gold and iridium, etc. Therefore, it is occasion to consider impact of milling and investigate the change of modified devices parameters.

2 INSTRUMENTATION

2.1 CURRENT-VOLTAGE CHARACTERISTICS

Experimental set-up for current-voltage measurement is shown in Figure 1. The sample is placed in the box between large aluminum electrodes and isolation plate to avoid electrode shunting. Metal box provides basic shielding from the surrounding electromagnetic noise and daylight. Sample temperature is controlled by source meter Keithley 2510-AT connected to Peltier's module with water cooling.

Source meters Keithley 2510-AT and 2420 are interconnected via 8-bit parallel multi-master interface bus standard IEEE-488.2 commonly called GPIB (General Purpose Interface Bus). Both devices are connected via GBIB/USB interface with PC equipped with Matlab. PC has installed software standard VISA (Virtual Instrument Software Architecture) for communication with hardware. Moreover, instruments are controlled by commands of standard SCPI (Standard Commands for Programmable Instruments). The bias voltage and current limit can be set in forward and reverse region.

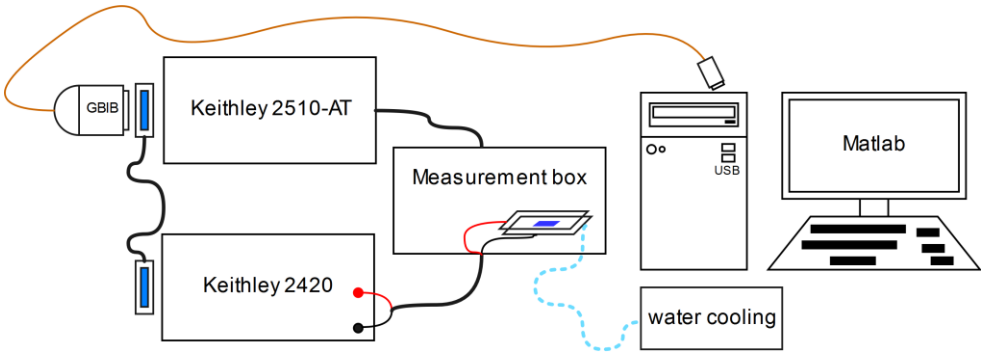

Figure 1: Set-up of current-voltage measurement system

2.2 FAR-FIELD IMAGING

For the far-field imaging high sensitivity CCD camera it is used. Camera silicon chip (KAF-3200ME) has resolution 3.2 MPx (2184×1472) and it is cooled with Peltier's module to minimize the sensor noise. Spectral range of used camera is from 300 nm to 1100 nm and optionally several optical filters can be applied. Solar cell under test is electrically biased and light emitted from defects is detected by camera. Camera is zoomed and focused to small area approximately 10x10 mm^2 to observe whole samples.

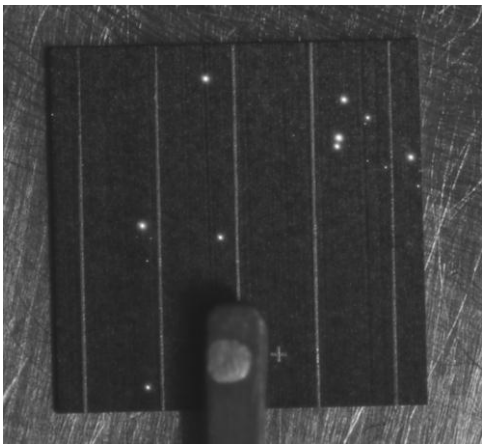

Figure 2: Light emission of defects on reversed bias solar cell, bias voltage U_r = 6.5 V, exposition time t = 10 s, temperature T = 297 K

2.3 SCANNING NEAR-FIELD MICROSCOPY

For localization defects in microscopic scale SNOM is used. It provides topography measurement and simultaneously is able to detect the weak optical signals from low-light emitting spots using photomultiplier tube (PMT). Principle is shown in

Figure 3a, monocrystalline silicon solar cell sample is reverse biased and light emitting spots on cell appears. Light emitting spots emits to all direction, only part of emitted light is detected by photocathode. When the scanning probe is placed between the light emitting spot and PMT photocathode, the probe forms a shadow that affects intensity of light detected on the PMT photocathode [8]. Emitted light is measured at every single step of the probe trajectory and finally the "shadow map" image is formed (

Figure 3b).

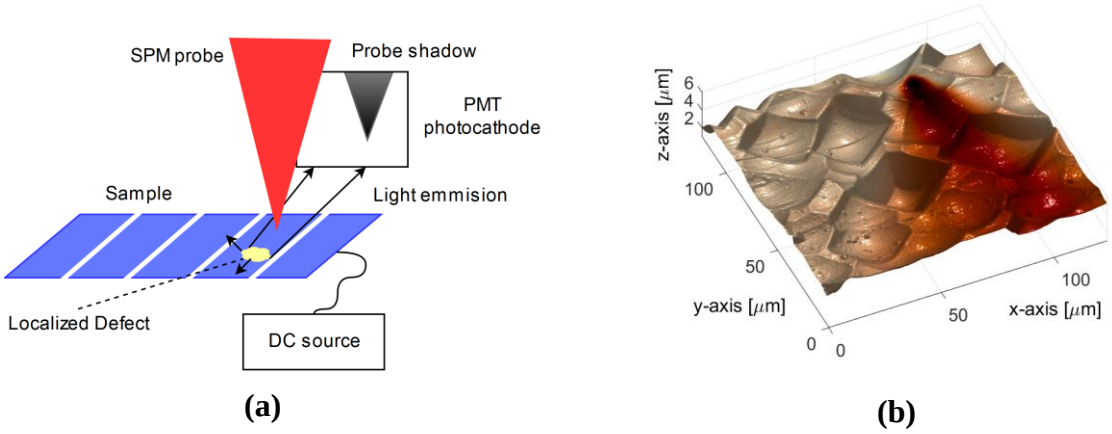

(a) **(b)**

Figure 3: (a) Principle of defect localization using SNOM, (b) Example of silicon solar cell topography with defect pointed by probe shadow

3 RESULTS

Five samples without defects were locally modified the same way by FIB. Milled volume was 3x3x7 μm^3 and also parameters of ion beam were the same for all the samples. SEM micrograph of milled areas is shown in Figure 4. The sizes of milling area were chosen with respect to the size of the typical defect. It should be noted that the *pn* junction was surely removed from milled area, but ions used for milling process were implanted to the substrate.

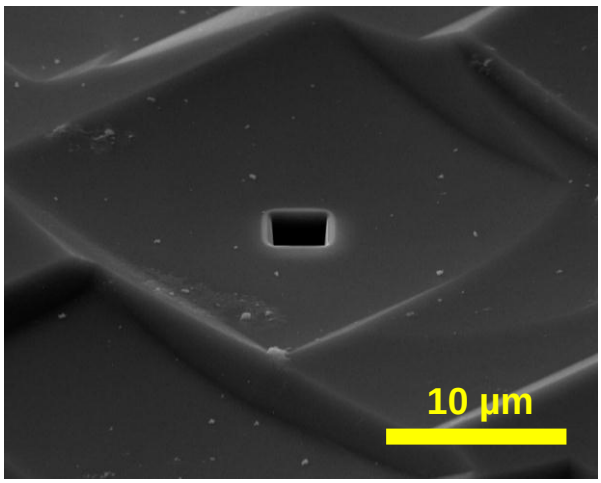

Figure 4: SEM image of ion milled area, tilt 55°

Newly created interface that crossing the junction, affect the sample electrical properties. Missing silicon atoms results in unpaired valence electrons on the interface (Figure 5) and thus form electrically active interface traps [9]. Moreover, it is known that implanted ions affect the crystal lattice and can also form amorphous layers.

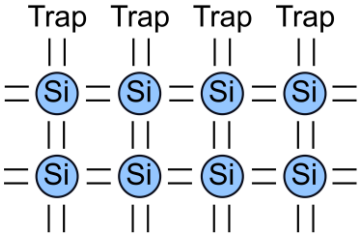

Figure 5: Silicon surface at dangling bond

3.1 MEASURED CHARACTERISTICS

I-V characteristics were measured in the dark environment and sample temperature was controlled. Differences in I-V characteristics before and after FIB show the excessive current flow through the milled junction area. From graphs shown in

Figure 6 it is obvious that dangling bonds of silicon surface and implanted ions form electrically active interface that acts like defect.

The reversed current after modification is significantly higher, compared to before curve, for the voltage above threshold $U_r = 5$ V, see

Figure 6 (a). Similar behavior was observed for all measured samples. The curves in Fig. 6 (b) show addition of current after FIB process as a function of voltage. Future investigation will be normalized to perimeter of milled area after repeated milling.

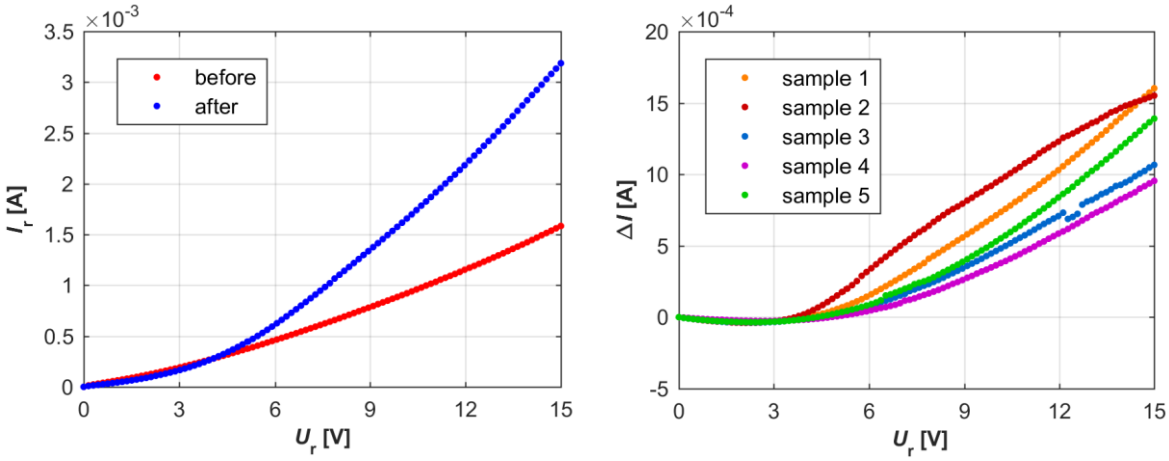

Figure 6: (a) Reverse biased *I-V* curve for sample 3 before and after FIB milling, $T = 300$ K (b) Reverse biased ΔI-V curve, $T = 300$ K

4 CONCLUSION

Method for detection and localization of specific type defects was shown. Although the FIB can be used for defect elimination, it was experimentally shown that this modification will form new defects in milled area. Excess current flowing through these areas is observable only for the bias voltages higher than threshold value. For the voltages lower than $U_r = 3$ V there are only minor differences in measured curves before and after FIB process. These are preliminary results; future inves-

tigation will deal with modifying size of milling area and ion beam parameters for the complex result and better explanation of the defects nature.

ACKNOWLEDGEMENT

This work was supported by the Internal Grant Agency of Brno University of Technology, grant No. FEKT-S-17-4626.

REFERENCES

[1] J.-P. Colinge and C. A. Colinge, *Physics of Semiconductor Devices*. Springer Science & Business Media, 2005.

[2] M. A. Green *et al.*, "Solar cell efficiency tables (version 49)," *Prog. Photovolt. Res. Appl.*, vol. 25, no. 1, pp. 3–13, Jan. 2017.

[3] O. Breitenstein, J. P. Rakotoniaina, M. H. Al Rifai, and M. Werner, "Shunt types in crystalline silicon solar cells," *Prog. Photovolt. Res. Appl.*, vol. 12, no. 7, pp. 529–538, Nov. 2004.

[4] S. Ostapenko, I. Tarasov, J. P. Kalejs, C. Haessler, and E.-U. Reisner, "Defect monitoring using scanning photoluminescence spectroscopy in multicrystalline silicon wafers," *Semicond. Sci. Technol.*, vol. 15, no. 8, p. 840, 2000.

[5] L. Grmela, P. Škarvada, P. Tománek, R. Macků, and S. Smith, "Local investigation of thermal dependence of light emission from reverse-biased monocrystalline silicon solar cells," *Sol. Energy Mater. Sol. Cells*, vol. 96, pp. 108–111, Jan. 2012.

[6] P. Škarvada *et al.*, "A variety of microstructural defects in crystalline silicon solar cells," *Appl. Surf. Sci.*, vol. 312, pp. 50–56, Sep. 2014.

[7] S. Reyntjens and R. Puers, "A review of focused ion beam applications in microsystem technology," *J. Micromechanics Microengineering*, vol. 11, no. 4, p. 287, 2001.

[8] P. Škarvada, Tománek, L. Grmela, and S. J. Smith, "Microscale localization of low light emitting spots in reversed-biased silicon solar cells," *Sol. Energy Mater. Sol. Cells*, vol. 94, pp. 2358–2361.

[9] E. Cartier, J. H. Stathis, and D. A. Buchanan, "Passivation and depassivation of silicon dangling bonds at the Si/SiO2 interface by atomic hydrogen," *Appl. Phys. Lett.*, vol. 63, no. 11, pp. 1510–1512, 1993.